

A scanning probe-based pick-and-place procedure for assembly of integrated quantum optical hybrid devices

Andreas W. Schell,^{1, a)} Günter Kewes,¹ Tim Schröder,¹ Janik Wolters,¹ Thomas Aichele,¹ and Oliver Benson¹
Nano-Optics, Institute of Physics, Humboldt-Universität zu Berlin, Newtonstraße 15, D-12489 Berlin, Germany

Integrated quantum optical hybrid devices consist of fundamental constituents such as single emitters and tailored photonic nanostructures. A reliable fabrication method requires the controlled deposition of active nanoparticles on arbitrary nanostructures with highest precision. Here, we describe an easily adaptable technique that employs picking and placing of nanoparticles with an atomic force microscope combined with a confocal setup. In this way, both the topography and the optical response can be monitored simultaneously before and after the assembly. The technique can be applied to arbitrary particles. Here, we focus on nanodiamonds containing single nitrogen vacancy centers, which are particularly interesting for quantum optical experiments on the single photon and single emitter level.

I. INTRODUCTION

In recent years, the integration of single quantum emitters into nanophotonic structures such as microcavities¹, optical antennas² or waveguides³ has attracted major interest in quantum and nano optics. Especially nitrogen vacancy (NV) defect centers in diamond crystals turned out to be stable and bright single-photon emitters even under ambient conditions^{4,5}. Due to the triplet ground state with electron spin decoherence times in the millisecond range, NV centers are also used as quantum memory systems and as nanomagnetic probes^{6,7}. Color centers occur naturally or can be artificially inserted into the diamond crystal by ion implantation^{8,9}. Combined with lithographic techniques, this top-down approach allows permanent integration of color centers into microcavities and waveguides^{10,11}. In contrast, diamond nanocrystals containing single defect centers can be coupled to photonic nanostructures to build hybrid quantum systems in a bottom-up approach. For positioning the nanocrystals with nanometer precision a scanning electron microscope (SEM) with a manipulator^{12,13} or a scanning atomic force microscope (AFM)^{14–16} have been used to date.

Controlled pushing of nanometer-sized objects on a surface through the AFM tip has been demonstrated for the first time by Junno et al.¹⁷ Picking up of metallic nanoparticles can be achieved by using electrostatic forces¹⁸ or after chemical treatment of the AFM tip¹⁹. In previous experiments^{20–22} we were striving for a refined dip-pen technique²³ for assembly of fluorescent nanoparticles on a multitude of optical devices. In this paper, we now describe an easily adaptable pick-and-place procedure which is particularly suitable for precise positioning of diamond nanocrystals.

II. EXPERIMENTAL SETUP

The experimental setup (Figure 1 (a)) for our pick-and-place process consists of an inverse confocal microscope with an AFM (NanoWizard, JPK Instruments) atop. We used two different microscopes. One is a Zeiss Axiovert 200 (Figure 2 (a) and (b)), the other one was homebuilt (Figure 2 (c)). Additionally, a special holder was constructed to allow for AFM manipulation on more complex or fragile photonic structures, such as optical fibers (Figure 2 (d)). While the AFM is a tip scanner with three axes, the confocal microscope has a 2D piezo sample stage (either PXY 80 D12, piezosystem jena / PXY100 ID, piezosystem jena) and a piezo actuated z-axis objective positioning system (MIPOS 100, piezosystem jena). In this way, the nanoparticle sample as well as the AFM tip can be positioned independently relative to the laser focus.

A sample was produced by spincoating of an ensemble of nanodiamonds from a solution on a glass coverslip. The solution is a suspension of centrifuge cleaned nanodiamonds (Microdiamant AG) in water with 0.02% polyvinyl alcohol. On such a sample individual nanodiamonds were pre-characterized prior to the pick up procedure. Light from a pulsed laser (LDH-P-FA-530, PicoQuant) with a wavelength of 532 nm and a repetition rate of 10 MHz was focussed on a nanodiamond via a high numerical aperture objective (UPlanSApo 60XO, Olympus / PlanApo 60XO, Olympus). Its fluorescence was dispersed by a grating spectrometer (SpectraPro-2500i, Acton) to identify a characteristic NV spectrum (see Figure 1 (c)). Autocorrelation measurements of the fluorescence were performed with the help of a Hanbury Brown and Twiss (HBT) setup consisting of a 50/50 beam splitter and two avalanche photodiodes (PDM Series, Micro Photon Devices / SPCM-AQR-14, Perkin Elmer). Time intervals between photons were measured with either a TimeHarp 200 or a PicoHarp 300 from PicoQuant. By evaluating the autocorrelation function $g^{(2)}(\tau)$ (see Figure 1 (b)) at $\tau = 0$ the number of emitting NV centers in the nanodiamond could be determined²⁴. Only nanodiamonds containing a single NV center, i.e., those with

^{a)}Electronic mail: andreas.schell@physik.hu-berlin.de

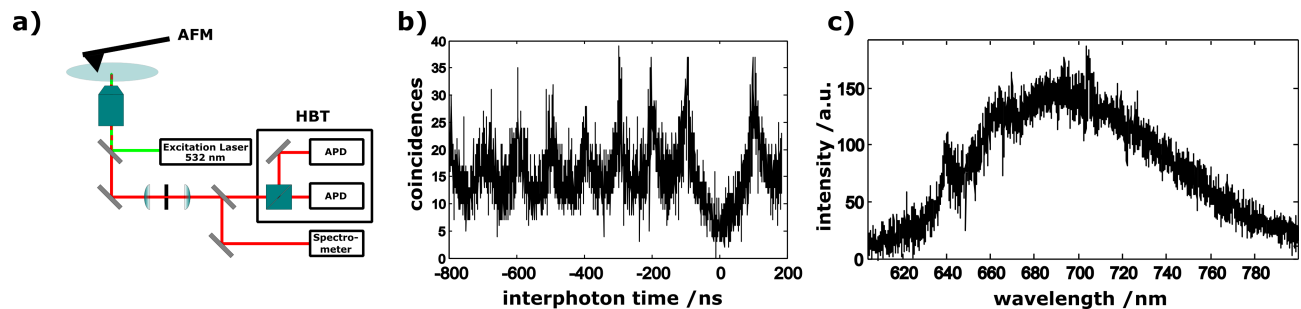


FIG. 1. (a) Schematics of the setup used to pre-characterize and pick up nanodiamonds. (b) Example of an autocorrelation measurement of fluorescence from an NV center in a nanodiamond showing pronounced antibunching. The repetition rate of the pulsed excitation laser at 532 nm was 10 MHz. (c) Spectrum of the same NV center with a zero phonon line peak at 639.6 nm.

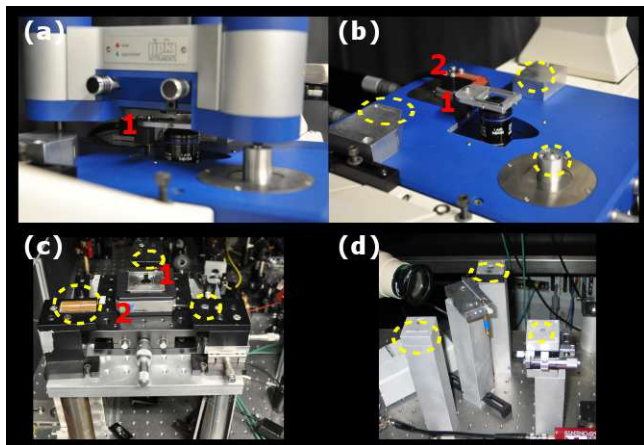


FIG. 2. Photograph the body of a Zeiss Axiovert 200 microscope converted to a confocal microscope with the AFM atop (a) and removed (b), respectively. (c) Top-view photograph of the homebuilt confocal microscope. (d) Detailed view of a special holder consisting of three posts for mounting the AFM to approach complex shaped items, e.g., an optical fiber. The dashed circles label the AFM mounts, 1 labels the sample holder and 2 labels the piezo sample scanner.

a vanishing peak at $g^{(2)}(0) = 0$ were used for the subsequent pick-and-place procedure.

A homebuilt nanosecond pulse counter was used for monitoring the optical signal and for converting the digital signal of the APDs to an analog voltage which was fed to the analog to digital converter of the AFM. This provides the opportunity to directly overlay topography and optical signal. The AFM was controlled with its standard software while homemade software written in Labview (National Instruments) and a multi-function data acquisition card (PCI-6014, National Instruments) were used to control the confocal microscope.

III. THE PICK-AND-PLACE PROCEDURE

The pre-characterized nanodiamond is placed into the optical focus of the confocal microscope and is identified with the AFM by scanning the tip over the focus in intermittent contact mode. In addition to the standard AFM images like topography and phase we also record the optical signal from the optical microscope versus tip position. To suppress the excitation light we used a longpass filter at $\lambda = 590$ nm. With the AFM approached we used an additional shortpass filter at $\lambda = 740$ nm to suppress the infrared AFM laser.

The optical signal consists of two contributions. Firstly, there is a constant fluorescence signal from the NV center in the laser focus. A second contribution stems from fluorescence of the AFM tip which depends on the position of tip relative to the focus. Thus, scanning the tip over the laser focus results in an AFM topography image together with an optical image of the focus area. Figure 3 (a,b) show the AFM topography and the optical image, respectively, with a single nanodiamond in the laser focus. In some cases (Figure 3 (b)) the fluorescence drops at the nanodiamond location. This is due to a modified scattering of the tip's fluorescence towards the collection optics of the confocal microscope when the tip is scanned across the nanodiamond. If the density of nanodiamonds on the substrate is sufficiently low, a single diamond nanoparticle can be identified in the laser focus unambiguously.

The pick up procedure is started by positioning the AFM tip above the nanodiamond. Then, the tip is pressed on the center of the particle in contact mode. A force of up to $1 \mu\text{N}$ is applied which is sufficient to attach the particle to the tip due to surface adhesion. Simultaneously the fluorescence is observed. If the nanodiamond is picked up successfully, the fluorescence signal drops to background level after the tip is retracted (see Figure 3 (c)). In order to ensure that the nanodiamond is picked up by the tip, and not only pushed out of the laser focus, the sample stage is used to scan the vicinity of the original nanodiamond position. If the pick up was not successful the tip is pressed on the nanodi-

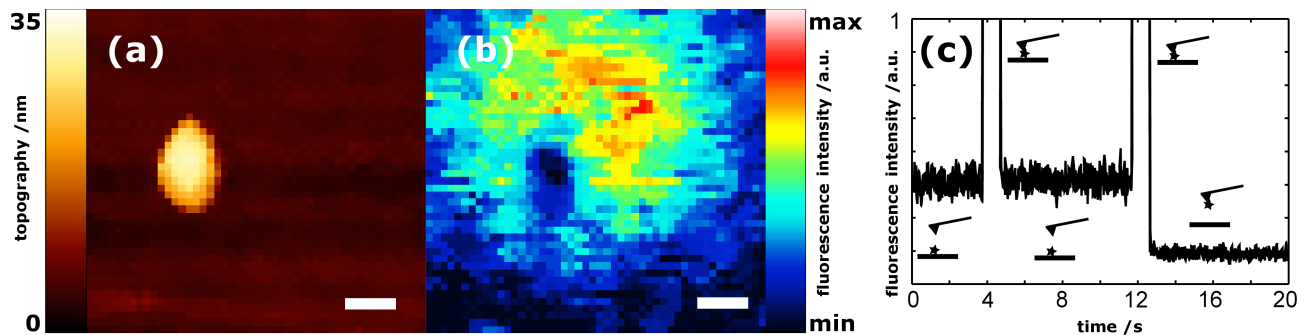


FIG. 3. (a) AFM topography image of a nanodiamond in the spot of a confocal microscope’s laser. (b) Optical image, i.e., detected fluorescence signal versus tip position. In this measurement the collected fluorescence is reduced when the tip scans across the diamond nanoparticle (see text). Scalebars in (a,b) are 100 nm. (c) Detected fluorescence signal when picking up the diamond. The fluorescence increases when the tip is at the sample surface. After a first unsuccessful attempt where the fluorescence had fully recovered the pick up procedure was repeated, and finally the nanodiamond was picked up indicated by a drop of the fluorescence signal to the background level.

amond again until it is finally picked up. From time to time, an additional topography image with the AFM in intermittent contact mode is taken in order to determine the diamond’s position. This is necessary, because the diamond sometimes moves a distance on the order of the tip radius when touched by the AFM tip. In our experiments a pick up was always possible, even if it could take a large number of approaches (sometimes over 50).

After being picked up the nanodiamond can be transferred to any structure accessible with the AFM. It is even possible to transport the whole AFM to another setup without losing the nanodiamond. If the new structure is not suitable for confocal microscopy with simultaneous AFM access, care has to be taken that the diamond can be clearly identified after it has been deposited. Therefore, a small area (e.g. $0.1 \mu\text{m}^2$) on the targeted structure is scanned by the AFM in intermittent contact mode. In this scanning process it is unlikely to lose the diamond as long as there are no sharp edges on the target surface. The diamond is then deposited by pressing the tip on the surface with a force of up to $1 \mu\text{N}$ and the area is scanned again. This is repeated until the nanodiamond appears on the topography image.

In contrast to the pick up process this is not always successful. Only approximately one third of the diamonds picked up could be placed again. We attribute this to nanodiamonds sticking at the side of the tip instead of the tip apex. When pressed to the surface, these nanodiamonds are pushed further along the side of the tip until they can not reach the surface anymore. Obviously, there is always a competition among adhesion between the nanoparticle and the tip and the nanoparticle and the target surface, respectively. When a diamond was lost, a new cantilever was used to make sure that the diamond deposited is really the one pre-characterized before.

A sketch of the whole procedure is given in Figure 4. The technique is presented here for nanodiamonds. In principle, it is possible to extend it to any other nanoparticle since it only relies on surface adhesion and does not

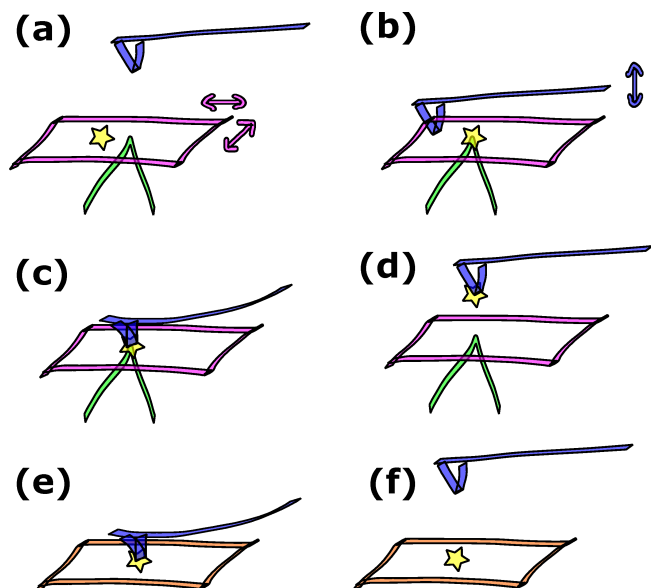


FIG. 4. Scheme of the nanodiamond pick-and-place procedure. (a) The sample is scanned in the confocal microscope in order to find and optically characterize a nanodiamond. (b) The AFM tip is scanned across the focal region of the microscope to identify the chosen nanodiamond. (c) The tip is pressed on the nanodiamond. (d) The nanodiamond sticks to the tip. (e) The tip is pressed on a new structure to deposit the nanodiamond. (f) The diamond is positioned at the desired position.

require a chemical functionalization of the surfaces.

The pick-and-place procedure has to be refined if the targeted structures have sharp edges near the desired nanoparticle position. Examples are photonic crystal cavities²⁰ or photonic crystal fibers²¹. In this case, a two-step process is needed. The nanodiamond is first placed on a smoother area of the target structure. Then, an AFM topography image of the targeted region can be taken with the bare tip. In this way the risk of losing

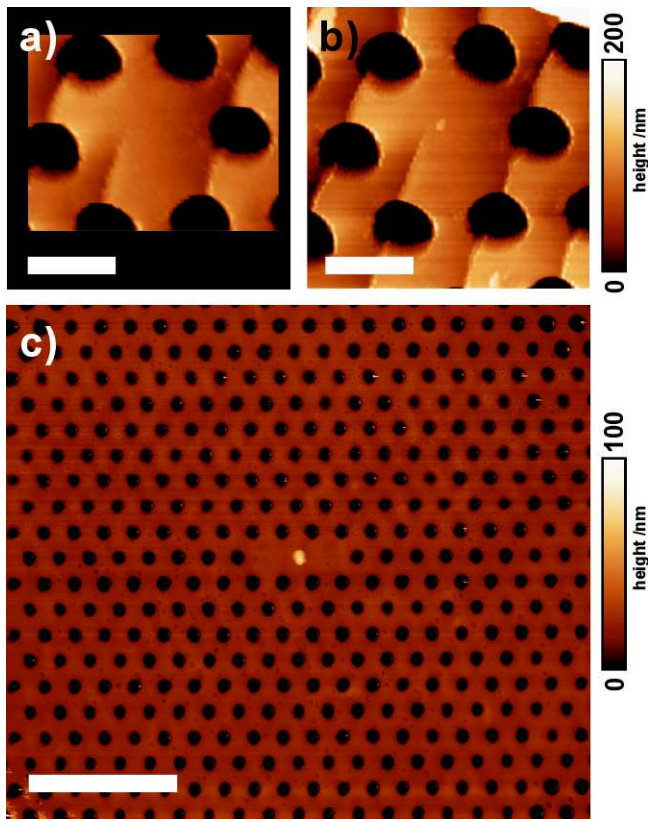


FIG. 5. (a) and (b) AFM image of the core of a photonic crystal fiber before and after placing a nanodiamond, respectively. (c) A nanodiamond placed inside a gallium phosphide photonic crystal membrane cavity. The thickness of the free-standing membrane is approx. 60 nm. All scalebars are 1 μ m.

the nanodiamond when scanning tip and nanodiamond across sharp edges is avoided. With the targeted region well identified via the AFM topography image, the diamond is finally transferred to its target position by a second pick-and-place process. One disadvantage of this two-step process is the lack of optical control during the second pick up, what makes the whole process more time consuming, since after each try an AFM scan has to be performed in order to determine if the nanodiamond has been picked up. Two examples of nanodiamonds transferred with the two step process are shown in Figure 5 (a-c).

In principle, the pick-and-place procedure can be performed with any AFM cantilever, but for optimum performance, there are some requirements. First, it is advantageous for the cantilever tip to have a radius of curvature which is large, since the probability for the nanodiamond to attach to the tip's side rather than to its apex decreases with increasing radius. On the other hand, the radius of curvature has to be sufficiently small to identify single nanoparticles in an AFM topography image. Second, ductile tips are preferred because they do not break when being pressed multiple times on the sample. Third, the tip material is important, because the adhe-

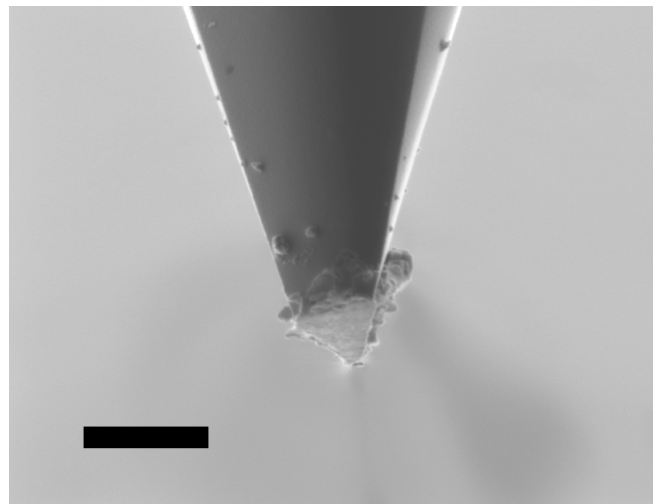


FIG. 6. SEM image of Pt/Ti coated cantilever used for the pick-and-place procedure. The tip has flattened by being pressed on the surface in order to pick up a nanodiamond. Scalebar is 1 μ m.

sion forces strongly depend on the involved materials²⁵. To our experience these requirements are best met by metal coated silicon tips, which are commercially available (we used Au and Pt/Ti coated cantilevers from MicroMasch). These tips seldom break compared to uncoated ones, have a higher radius of curvature (approx. 40 nm) and it is possible to deform them by pressing them on the substrate or on a nanodiamond. An example for a used Pt/Ti coated tip can be seen in Figure 6.

IV. CONCLUSION

In conclusion, we have described a versatile technique to transfer nanoparticles, in particular nanodiamonds, with nanometer precision even between different samples. This technique allows positioning of specific nanoparticles to a variety of structures, overcoming high densities and random positioning during a spin-coating operation. The method is particularly attractive for samples where a standard spin-coating of nanoparticles does not work for geometrical reasons, like optical fibers²¹ and nanocavities¹⁵. Moreover the presented technique can be used at ambient environments and can be combined with optical monitoring in contrast to manipulation in a SEM.

ACKNOWLEDGEMENT

We acknowledge financial support from DFG through project IQoSuPla (AI 92/3) and thank Max Schoengen for taking the SEM picture in Figure 6.

¹K. J. Vahala, *Nature* **424**, 839 (2003).

²P. Mühlischlegel, H.-J. Eisler, O. J. F. Martin, B. Hecht, and D. W. Pohl, *Science* **308**, 1607 (2005).

- ³J. L. O'Brien, A. Furusawa, and J. Vuckovic, *Nature Photon.* **3**, 687 (2009).
- ⁴C. Kurtsiefer, S. Mayer, P. Zarda, and H. Weinfurter, *Phys. Rev. Lett.* **85**, 290 (2000).
- ⁵R. Brouri, A. Beveratos, J.-P. Poizat, and P. Grangier, *Opt. Lett.* **25**, 1294 (2000).
- ⁶G. Balasubramanian, P. Neumann, D. Twitchen, M. Markham, R. Kolesov, N. Mizuochi, J. Isoya, J. Achard, J. Beck, J. Tissler, V. Jacques, P. R. Hemmer, F. Jelezko, and J. Wrachtrup, *Nature Mater.* **8**, 383 (2009).
- ⁷G. Balasubramanian, I. Y. Chan, R. Kolesov, M. Al-Hmoud, J. Tisler, C. Shin, C. Kim, A. Wojcik, P. R. Hemmer, A. Krueger, T. Hanke, A. Leitenstorfer, R. Bratschitsch, F. Jelezko, and J. Wrachtrup, *Nature* **455**, 648 (2008).
- ⁸J. Meijer, B. Burchard, M. Domhan, C. Wittmann, T. Gaebel, I. Popa, F. Jelezko, and J. Wrachtrup, *Appl. Phys. Lett.* **87**, 261909 (2005).
- ⁹J. Meijer, S. Pezzagna, T. Vogel, B. Burchard, H. Bukow, I. Rangelow, Y. Sarov, H. Wiggers, I. Plmel, F. Jelezko, J. Wrachtrup, F. Schmidt-Kaler, W. Schnitzler, and K. Singer, *Appl. Phys. A* **91**, 567 (2008).
- ¹⁰T. M. Babinec, J. T. Choy, K. J. M. Smith, M. Khan, and M. LonCar, *J. Vac. Sci. Technol. B* **29**, 010601 (2011).
- ¹¹K.-M. C. Fu, C. Santori, P. E. Barclay, I. Aharonovich, S. Praver, N. Meyer, A. M. Holm, and R. G. Beausoleil, *Appl. Phys. Lett.* **93**, 234107 (2008).
- ¹²E. Ampem-Lassen, D. A. Simpson, B. C. Gibson, S. Trpkovski, F. M. Hossain, S. T. Huntington, K. Ganesan, L. C. Hollenberg, and S. Praver, *Opt. Express* **17**, 11287 (2009).
- ¹³T. van der Sar, E. C. Heeres, G. M. Dmochowski, G. de Lange, L. Robledo, T. H. Oosterkamp, and R. Hanson, *Appl. Phys. Lett.* **94**, 173104 (2009).
- ¹⁴S. Schietinger, M. Barth, T. Aichele, and O. Benson, *Nano Lett.* **9**, 1694 (2009).
- ¹⁵M. Barth, N. Nüsse, B. Löchel, and O. Benson, *Opt. Lett.* **34**, 1108 (2009).
- ¹⁶A. Huck, S. Kumar, A. Shakoor, and U. L. Andersen, *Phys. Rev. Lett.* **106**, 096801 (2011).
- ¹⁷T. Junno, K. Deppert, L. Montelius, and L. Samuelson, *Appl. Phys. Lett.* **66**, 3627 (1995).
- ¹⁸J. Toset, I. Casuso, J. Samitier, and G. Gomila, *Nanotechnology* **18**, 015503 (2007).
- ¹⁹Y. Tanaka and K. Sasaki, *Appl. Phys. Lett.* **96**, 053117 (2010).
- ²⁰J. Wolters, A. W. Schell, G. Kewes, N. Nüsse, M. Schoengen, H. Döscher, T. Hannappel, B. Löchel, M. Barth, and O. Benson, *Appl. Phys. Lett.* **97**, 141108 (2010).
- ²¹T. Schröder, A. W. Schell, G. Kewes, T. Aichele, and O. Benson, *Nano Lett.* **11**, 198 (2011).
- ²²A. W. Schell, G. Kewes, T. Hanke, A. Leitenstorfer, R. Bratschitsch, O. Benson, and T. Aichele, *Opt. Express* **19**, 7914 (2011).
- ²³Y. Wang, Y. Zhang, B. Li, J. Lu, and J. Hu, *Appl. Phys. Lett.* **90**, 133102 (2007).
- ²⁴Y. Sonnefraud, A. Cuche, O. Faklaris, J.-P. Boudou, T. Sauvage, J.-F. Roch, F. Treussart, and S. Huant, *Opt. Lett.* **33**, 611 (2008).
- ²⁵T. Eastman and D.-M. Zhu, *Langmuir* **12**, 2859 (1996).